A-TYPE MAGMATISM IN THE SIERRAS OF MAZ AND ESPINAL: A NEW RECORD OF RODINIA BREAK-UP IN THE WESTERN SIERRAS PAMPEANAS OF ARGENTINA

Fernando Colombo[1*], Edgardo G. A. Baldo[1], César Casquet[2], Robert J. Pankhurst[3], Carmen Galindo[2], Carlos W. Rapela[4], Juan A. Dahlquist[1] and C. Mark Fanning[5]

[1]Departamento de Geología – FCEFyN - Universidad Nacional de Córdoba. Vélez Sarsfield 1611 (X5016GCA) Córdoba - Argentina
[2]Departamento de Petrología y Geoquímica, Universidad Complutense, 28040 Madrid - Spain
[3]British Geological Survey, Keyworth, Nottingham NG12 5GG - England
[4]Centro de Investigaciones Geológicas, Universidad Nacional de La Plata (1900) La Plata - Argentina
[5]Research School of Earth Sciences, The Australian National University, Canberra - Australia

[*]: corresponding author. e-mail fcolombo@com.uncor.edu Fax: ++54-351-4334139

Abstract

Two orthogneisses have been recognized in the sierras of Espinal and Maz (Western Sierras Pampeanas, NW Argentina) that were emplaced within a Grenvillian metasedimentary sequence. Microcline, plagioclase and quartz are the main rock-forming minerals, with accessory zircon, apatite-(CaF), magnetite, biotite (Fe/(Fe+Mg) = 0.88-0.91), ferropargasite (Fe_{total}/(Fe_{total} + Mg) = 0.88-0.89), titanite (with up to 1.61 wt.% Y_2O_3) and an REE-rich epidote. REE-poor epidote and zoned garnet (Ca and Fe^{3+}-rich) are metamorphic minerals, while muscovite, carbonates and chlorite are secondary phases. Texture is mylonitic.

Two representative samples are classified as granite (from Sierra de Espinal) and granodiorite/tonalite (from Sierra de Maz) on the grounds of immobile trace elements. Some trace element contents are rather high (Zr: 603 and 891 ppm, Y: 44 and 76 ppm, 10000*Ga/Al: 2.39-3.89) and indicate an affiliation with A-type granites (more specifically, the A_2 group). Both samples plot in the field of within-plate granites according to their Y and Nb contents.

Concordant crystallization ages (zircon U-Pb SHRIMP) are 842 ± 5 and 846 ± 6 Ma respectively. $^{87}Sr/^{86}Sr_{i\ (845)}$ ratios are 0.70681 and 0.70666; $\varepsilon Nd_{i\ (845)}$ values are -1.5 and +0.3 and depleted mantle Nd model ages ($2T_{DM}$*) are 1.59 and 1.45 Ga respectively. These values indicate the involvement of an isotopically evolved source. $2T_{DM}$* values are compatible with the presence of inherited zircon crystals of up to 1480 Ma in one of the rocks, thus implying that magmas incorporated material from Mesoproterozoic continental source. This is also indicated by the relatively high contents of Y, Ga, Nb and Ce compared to magmas derived from sources similar to those of oceanic-island basalts.

These orthogneisses represent a period of extension at ca. 845 Ma affecting the Western Sierras Pampeanas continental crust that was already consolidated after the Grenvillian orogeny (1.2 – 1.0 Ga). They are thus a record of the early stages of Rodinia break-up. Metamorphic conditions during the subsequent Famatinian orogenic cycle (ca. 420 Ma, SHRIMP U-Pb on zircon) attained 7.7 ± 1.2 kbar and 664 ± 70ºC.

Keywords: Rodinia; U-Pb SHRIMP dating; anorogenic magmatism; Mesoproterozoic; Western Sierras Pampeanas; Argentina.

Introduction

The Sierras Pampeanas in northwestern Argentina constitute large exposures of pre-Mesozoic crystalline basement in the foreland of the the Central Andes (Fig. 1A). They record a complex tectonomagmatic history from the Mesoproterozoic to the Late Paleozoic that has not yet been completely deciphered. In the Western Sierras Pampeanas evidence for a reworked Grenville-age basement was firmly demonstrated by McDonough et al. (1993). This basement has since been considered the counterpart of the Grenville orogen along the southern Appalachian margin of Laurentia, which drifted away in the late Neoproterozoic to early Paleozoic to finally dock against the proto-Andean margin of Gondwana in the Ordovician. Whether this process involved an allochthonous exotic terrane, i.e., the Precordillera terrane hypothesis (for a review see Thomas and Astini, 2003, Ramos, 2004), or para-authoctonous translation along the proto-Andean margin of Gondwana (e.g., Finney, 2007; Casquet et al. 2008a), remains a matter of dispute. However all authors agree that the Western Sierras Pampeanas Grenville-age terranes were contiguous to Laurentia by the end of Rodinia amalgamation at ca. 1.0 Ga. Moreover Casquet et al. (2008b) raised the hypothesis that, at the onset of the Grenvillian orogeny, the Western Sierras Pampeanas Grenvillian terranes were part of a larger continental mass that embraced other Meso- to Paleoproterozoic outcrops such as the Arequipa block in southern Peru and northern Chile. This view opens new ways to interpret the Proterozoic history of southern South America (Rapela et al., 2007).

Rodinia is the name given to a hypothetical supercontinent that comprised almost all continental masses on Earth during the late Mesoproterozoic. Geological evidence for the existence and evolution of such supercontinent has been growing since the early 1990's (e.g., Hoffman, 1991; Dalziel, 1991; Moores, 1991; see Li et al., 2008 for a review), but consensus is still lacking on issues such as the number of participating cratons, their relative positions and the chronology of the assembly and subsequent break-up of Rodinia. Rodinia break-up and dispersal began around 900 Ma ago or even earlier (e.g., Cordani et al., 2003), but evidence of widespread rifting associated with mantle plumes occurred much later, spanning the time interval between 825 and 740 Ma (Li et al., 2008).

Evidence for Rodinia break-up in the Western Sierras Pampeanas was first recognized in the Sierra de Pie de Palo (Fig. 1A). Here A-type orthogneisses hosted by reworked Grenvillian basement yielded a zircon U-Pb SHRIMP age of ca. 774 Ma. Protoliths were interpreted as resulting from an anorogenic magmatic event during early rifting of Rodinia (Baldo et al., 2006).

This contribution deals with a newly recognized anorogenic magmatic event at ca. 845 Ma in the sierras of Maz and Espinal (Fig. 1A) which records a still earlier event of Rodinia break-up. It thus adds to understanding of the Rodina break-up process in this part of Western Gondwana both in time and paleogeography.

Geological setting

The sierras of Maz and Espinal (Fig.1) were first described by Kilmuray and Dalla Salda (1971). Basement outcrops in the area, including those of the adjacent Sierra de Ramaditas and Villa Castelli massif, consist of metamorphic rocks with sedimentary

and igneous protoliths intruded by a Lower Ordovician suite of metaluminous and peraluminous granites that occurs east of the sierras, near Villa Castelli (Dahlquist et al 2007) (Fig.1). The basement outcrops are covered by Late and post-Paleozoic sedimentary rocks in angular unconformity. Westward high-angle thrusting during the Andean orogeny led to superposition of the basement blocks over the sedimentary cover (Jordan and Almendinger, 1986).

In the basement of the sierras of Maz and Espinal three domains separated by first order shear zones and faults (Fig. 1-B) were distinguished on the basis of field, geochronology and isotope composition evidence (Casquet et al., 2006, 2008 b). The Eastern Domain, consisting for the most part of high grade rocks, i.e., garnet-sillimanite migmatitic gneisses with subordinate marbles and amphibolites, is younger than 1.0 Ga. Metamorphism took place during the Ordovician-Silurian Famatinian orogeny at ca. 440 Ma (see also Lucassen and Becchio, 2003). The Central Domain (also known as the Maz terrane) consists of medium-grade (kyanite-sillimanite-garnet-staurolite schists, quartzites, amphibolites and marbles) to high-grade intermediate-to-ultrabasic meta-igneous rocks and metasedimentary rocks that underwent a Grenvillian-age orogeny starting at ca. 1.2 Ga (Porcher et al., 2004; Casquet et al., 2006). Massif-type anorthosites of ca. 1070 Ma are restricted to the Maz terrane. Anorthosites also show evidence for Famatinian metamorphic rejuvenation (431 ± 40 Ma) throughout the Maz terrane (Casquet et al., 2005). Moreover, metamorphic and geochronological discontinuities within the Maz terrane suggest that it is in fact composed of a number of slivers separated by shear zones of unknown age, probably Famatinian. The Western Domain consists again of metasedimentary rocks younger than ca. 1.0 Ga that underwent Famatinian metamorphism. One sequence of rocks composed of thick marble beds, calcic semipelitic schists and quartzites is probably equivalent to the late Neoproterozoic Difunta Correa metasedimentary sequence of the Sierra de Pie de Palo, and to isotopically equivalent rocks of the Sierra de Umango (Varela et al. 2001, Galindo et al. 2004, Rapela et al. 2005). Most rocks within this domain are low-grade but high-grade rocks are locally found. A recently described ca. 0.57 Ga alkaline syenite-carbonatite complex (Casquet et al., 2008 c) occurs in the eastern margin of the Sierra of Maz.

Figure 1 should appear about here

Two orthogneisses have been found that have provided almost the same crystallization age of ca. 845 Ma (see below). Both are foliated sheeted bodies concordant with the external foliation and bedding. Field evidence suggests that the protoliths were intrusive and not tectonically emplaced. The first, in the Sierra of Maz (fig. 2-A), is a ca. 100m thick body of leucocratic mylonitic augen-gneiss with streaks of mafic minerals and concordant stretched pegmatites; the fabric is S=L. It is hosted by whitish quartzites, sillimanite-garnet gneisses and garnet amphibolites that are assigned on the basis of Nd model ages (Casquet et al., 2006) to the Western Domain referred to above. This domain underwent Famatinian metamorphism only. The second, in the Sierra del Espinal (fig. 2-B), is a mylonitic augen-gneiss hosted by a sequence of kyanite-staurolite-garnet schists, amphibolites, marbles and quartzites belonging to the Maz terrane (Casquet et al., 2006). The extent of this body is unknown, as only a section some 20 m thick is visible along one creek. This sequence underwent medium-grade Grenvillian metamorphism and a low-grade rejuvenation attributed here to the Famatinian orogeny (see below).

Figure 2 should appear about here

Sampling and analytical methods

Two samples were collected that are representative of the two orthogneisses: MAZ-6037 was taken from an outcrop along the Maz Creek (29º11´20´´W - 68º28´48´´S). ESP-7066 was collected on the western slopes of the Sierra del Espinal, close to Puesto Villalba (29º05´23´´W-68º31´40´´S) (Fig. 1B).

Electron-microprobe analyses were performed on sample MAZ-6037 and on a host amphibolite (MAZ-12046), the latter for estimation of metamorphic conditions, at the Complutense University, Madrid (Supplementary data files obtainable from the Precambrian Research Data Repository).

Whole-rock powders of ESP-7066 and of a further sample of the MAZ orthogneiss (MAZ-12040) were analysed by ActLabs (Canada) for major elements (ICP) and trace elements (ICP-MS) (4-Lithoresearch code) (Table 1).

Rb–Sr and Sm–Nd isotope determinations were carried out at the Geochronology and Isotope Geochemistry Center of the Complutense University (Madrid, Spain) on an automated multicollector VG® SECTOR 54 mass spectrometer. Analytical uncertainties are estimated to be 0.01% for $^{87}Sr/^{86}Sr$, 0.006% for $^{143}Nd/^{144}Nd$, 1% for $^{87}Rb/^{86}Sr$, and 0.1% for $^{147}Sm/^{144}Nd$. Replicate analyses of the NBS-987 Sr-isotope standard yielded an average $^{87}Sr/^{86}Sr$ ratio of 0.710227±0.00004 (n=10) and La Jolla Nd-isotope standard yielded an average $^{143}Nd/^{144}Nd$ of 0.511844±0.00002 (n=10). Errors are quoted throughout as two standard deviations from measured or calculated values (Table 2).

U-Th-Pb zircon dating was performed on the two samples at the Research School of Earth Sciences, The Australian National University, Canberra, Australia, using SHRIMP RG (MAZ-6037) and SHRIMP II (ESP-7066). Separated zircons were mounted in epoxy resin together with chips of the FC1 Duluth Gabbro reference zircon. Reflected and transmitted light photomicrographs and cathodo-luminescence (CL) SEM images were used to decipher the internal structures and to target specific areas within the zircons. Analytical methods followed Williams (1998, and references therein). U/Pb ratios were normalized relative to a value of 0.01859 for the FC1 reference zircon, equivalent to an age of 1099 Ma (see Paces and Miller, 1993) and data were reduced using the SQUID Excel macro of Ludwig (2001) (Supplementary SHRIMP data files are obtainable from the Precambrian Research Data Repository). Uncertainties are quoted at the 1-sigma level. ^{204}Pb-corrected data are presented, but it should be noted that this is not optimal for some of the low-U areas analysed, giving rise to large uncertainties in the radiogenic $^{207}Pb/^{206}Pb$ ratios and ages. All age calculations were carried out using Isoplot/Ex (Ludwig, 2003) and the resulting ages quoted in the text and figures are quoted with 95% confidence limits, including propagation of the uncertainties in the calibration of the U/Pb ratio of the reference zircons (0.40% for sample MAZ-6037 and 0.16% for ESP-7066).

Petrography and mineral chemistry

The Sierra del Espinal orthogneiss consists of quartz and microcline, with lesser amounts of plagioclase, opaque phases and very abundant muscovite and chlorite as

alteration products after biotite (Fig. 3-A and 3-B). Titanite and scarce zircon are the main accessory minerals. Because of the strong low-grade retrogression this rock was not further considered for electron microprobe analyses

The orthogneiss from the Sierra de Maz shows a mylonitic texture; microcline and plagioclase constitute rounded porphyroclasts, while quartz forms recrystallized ribbons (figure 3-C and 3-D). Microcline, plagioclase and quartz are the main rock-forming minerals and are inherited from the igneous paragenesis. Zircon, apatite, magnetite, biotite, amphibole (ferropargasite), titanite and an REE-rich epidote are accessory and except for some biotite and titanite are probably also inherited. However, garnet and an REE-poor epidote forming mantles around REE-rich epidote grains are metamorphic minerals, as are some biotite and titanite, and muscovite. The low Mn (7.87-1.74 wt% MnO) and high Ca (13.67-11.02 wt% CaO) contents are not characteristic of garnets of magmatic origin and are instead similar to metamorphic garnets from meta-granites (Le Goff and Ballevre, 1990, Kotopouli et al., 2000). Biotite and amphibole have high Fe/(Fe+Mg) ratios (0.88-0.91 and 0.88-0.89, respectively). Muscovite is of secondary origin (after biotite and feldspars) and is locally associated with opaque minerals. Irregular carbonate concentrations are locally observed.

Figure 3 should appear about here

Whole rock geochemistry

The two rocks are chemically different (Table 1). Unfortunately, identification of the gneiss protolith in terms of major element chemistry is subject to uncertainty because of the strong metamorphic overprint. A more realistic classification should be based on immobile elements such as HFS elements. On the $Zr/TiO_2*0.0001$ vs. Nb/Y plot (Winchester and Floyd, 1977), ESP-7066 is a rhyolite, i.e., granite, whereas MAZ-12040 plots in the field of rhyodacites/dacites, i.e. granodiorite to tonalite.

Table 1 should appear about here

Relying on HFS elements only, contents of Zr and Y are high in both rocks (603, 891 ppm and 44, 76 ppm, respectively). However, Nb and Ce are not so notably enriched (24, 27 ppm; 180, 97 ppm, respectively), although their values exceed those considered usual for fractionated I- and S-type granites (as compiled by Whalen et al., 1987) and are more typical of A-type granitoids. In fact values of 10000*Ga/Al are 2.39 and 3.89, respectively, i.e., close to or above the value of 2.6 recommended by Whalen et al. (1987) to distinguish A-type granitoids. On a Zr+Nb+Ce+Y diagram (Eby, 1990) the two rocks plot in the field of A-type granitoids (Fig. 4-A). On the other hand, contents of mobile elements such as Rb (low: 54-74 ppm), Sr (moderate: 97-232 ppm) and Ba (high: 1051-1787 ppm) are more typical of non-evolved granitoids. Normalized REE patterns are slightly fractionated (La_N/Lu_N = 13 and 4 respectively), with REE concentrations close to 100 times chondritic values (Fig. 4-B). The Eu anomaly is negative and moderate (0.64) in ESP-7066 and slightly positive (1.09) in MAZ-12040.

Both samples plot in the field of within-plate granites close to the field of volcanic-arc granites on discriminant diagrams based on relative abundances of Ta, Y, Yb, Nb, Hf and Rb (Pearce et al., 1984; Harris et al., 1986). Moreover, the two samples belong to the A_2 group as defined by Eby (1992), which represents magmas derived from

continental crust that has been through a cycle of subduction-zone or continent-continent collision magmatism (Figs 4-C and D).

Figure 4 should appear about here

Isotope composition

$^{87}Sr/^{86}Sr_i$ ratios at 845 Ma – the probable crystallization age (see below) – are 0.70681 and 0.70666 for MAZ 12040 and ESP-7066 respectively (Table 2). εNd_i values at the age of 845 Ma are +0.32 to – 1.5. Depleted mantle 2-stage Nd model ages ($2T_{DM}$) (De Paolo et al., 1992) are 1.45 and 1.59 Ga (Table 2). Sr and Nd isotope initial ratios are evidence that an isotopically moderately evolved source contributed to the magma composition. Moreover, Nd model ages suggest that this source might be sought in underlying Mesoproterozoic continental crust. This interpretation is reinforced by zircon data below. Whether a juvenile component was also involved in the magma composition cannot be confirmed with the available information.

Table 2 should appear about here

U-Pb SHRIMP geochronology

Zircons from MAZ-6037 are elongate to sub-equant, euhedral to sub-round grains or fragments that are generally between 200 to 300 μm in length. The CL images show a dominantly oscillatory-zoned internal structure, with many grains having a thin, <10μm bright CL rim (Fig. 5-A). Some grains show a more complex internal structure, with central areas of oscillatory zonation overgrown by a less clearly oscillatory zoned zircon, in turn overgrown by the very thin bright CL outermost rim for which no reliable analyses could be obtained. Thirty areas were analysed on 27 zircon grains (data obtainable from the Precambrian Research Data Repository). The Pb peaks were not correctly centred during the analyses of grains 5 and 6 and so no data is presented for these. The outer rim and core areas were analysed on grain 1 and both yield $^{207}Pb/^{206}Pb$ ages that are within uncertainty. The 28 analyses presented in the Data Repository are a mixture of both the inner and outer areas of grains, both types yielding Th/U ratios that are in the usual range recorded by igneous zircon (0.3–0.7). Furthermore, on the Wetherill concordia plot (Fig. 5-B) it can be seen that the majority of data lie within uncertainty of concordia and there is no consistent difference between analyses of these two zircon types. Some dispersion is evident and this probably results from correction errors associated with very small amount of radiogenic Pb. Twenty-two of the 28 analyses yield a self-consistent Concordia age (as in Ludwig, 2001) of 846 ± 6 Ma (MSWD = 1.4) and this constrains the crystallisation age of the dominant zoned igneous zircon. The fact that both inner and outer zoned components are within uncertainty at ca. 846 Ma indicates that they are coeval to within the uncertainty of SHRIMP analysis.

The zircons from sample ESP-7066 constitute a more heterogeneous population than those described above. The grains are mostly ~200 μm in length, but are more clearly sub-round, with a few subhedral, and under transmitted light they have clearly been more affected by a metamorphic event. The CL images show a range of complex structures. Whilst many show oscillatory zonation, there are older central cores to some grains, and more homogeneous embayments of low-luminescence metamorphic zircon in others (Fig. 5-C). This complexity is highlighted in the U-Pb data, with 17 analyses

on 14 zircon grains (see table in Data Repository). Two analyses of the presumed metamorphic embayments on grains 4 and 7 yield $^{206}Pb/^{238}U$ ages of ca. 420 Ma, consistent with Paleozoic metamorphism. Older inherited cores and whole grains give ages of ~1480, ~1200 and ~1000 Ma (Fig 5-C). The dominant oscillatory-zoned zircons yield a concordant group of analyses with a Concordia age of 842 ± 5 Ma (MSWD =2.0, 9 analyses, Fig. 5-D). This ca. 842 Ma igneous zircon can be seen to enclose older components (both igneous and metamorphic), and in turn is itself rimmed and embayed by the ca. 420 Ma metamorphic zircon.

The two samples thus provide crystallization ages that are coincident within error at ca. 845 Ma, i.e., Early Cryogenian, according to the International Stratigraphic Chart (International Commission on Stratigraphy, 2008). Both have been affected by metamorphism which, at least in the case of ESP-7066, is shown to be Silurian.

Figure 5 should appear about here

Conditions of metamorphism

Peak metamorphic P-T conditions were assessed for the Maz site to contribute to a better knowledge of the orthogneisses petrology. Using of multivariate equilibria procedure was however hampered by the garnet composition, which is very rich in Ca and Fe, and outside the range of thermodynamic models. Therefore, the best estimate of metamorphic P-T conditions is obtained from the host rocks.

Calculations were made on a para-amphibolite close to the orthogneiss body (sample MAZ-12046) using THERMOCALC 3.1 (Powell and Holland, 1988. Garnet, amphibole, biotite, quartz, plagioclase and ilmenite constitute the dominant assemblage, while calcite, epidote and chlorite were formed on the retrograde path. Other minor phases include apatite, allanite and zircon. Syntectonic garnet displays a very slight zonation, with decreasing Mg (X_{Py} from 0.12 to 0.117-0.105) and Fe (X_{Alm} from 0.654 to 0.645-0.647) and increasing Ca (X_{Gro} from 0.177 to 0.182-0.190) and Mn (X_{Sps} from 0.048 to 0.053-0.059) from core to rim. Neither biotite nor amphibole is significantly zoned. Biotite has an average Mg# of 0.44. Amphibole (ferropargasite according to the classification of Leake et al., 1997) has Al_{Total} between 2.668 and 2.875 apfu and #Mg = 0.43. The average $Fe^{3+}/(Fe^{2+}+ Fe^{3+})$ ratio is 0.10. Plagioclase ranges from An_{54} to An_{67} (mineral compositions are obtainable from the Data Repository). Peak metamorphic conditions were: P = 7.7 ± 1.2 kbar and T = 664 ± 70º C.

Discussion

A-type magmatism is indicative of largely continental within-plate extensional settings (e.g., Eby, 1990, 1992; Bonin, 2007). Thus we infer that the A-type granitoids described here represent a period of extension at ca. 845 Ma (early Cryogenian) affecting the continental crust of the Western Sierras Pampeanas that was already consolidated after the Grenvillian orogeny. This magmatic event implies that rifting of the Western Sierras Pampeanas Grenvillian basement started earlier than previously established. The oldest crystallization age yet reported for anorogenic A-type granitoids in the Western Sierras Pampeanas is ca. 774 Ma (middle Cryogenian; Baldo et al., 2006). Compared to the juvenile isotope composition of the ca. 774 Ma Sierra de Pie de

Palo orthogneisses (Sr_i = 0.7005 to 0.7030, εNd = +4.1 to +4.9; Baldo et al., 2006), those of Maz and Espinal orthogneisses resulted from the involvement of an isotopically more evolved source. Moreover, depleted-mantle Nd model ages of up to 1.46 Ga and inherited zircon crystals of up to 1.48 Ga in sample ESP-7066 lead us to speculate that the ca. 845 Ma A-type magmatism at Maz, largely involved a Mesoproterozoic continental source. The latter is also indicated by the relatively high contents of Y, Ga, Nb and Ce compared to those of magmas directly derived from mantle sources (Eby, 1992).

Igneous rocks of uncertain chemical signature that might likewise correspond to the same anorogenic event referred to here have been recorded from other locations in the Western Sierras Pampeanas. Mulcahy et al. (2003) reported a U-Pb SHRIMP zircon age of 839 ± 10 Ma for an orthogneiss from the Sierra de la Huerta, southeast of the Sierra de Pie de Palo (Fig. 1). Vujovich et al. (2005) reported depleted mantle Nd model ages between 782 and 806 Ma for ortho-amphibolites from the Sierra de Umango, west of the Sierras of Maz and Espinal (Fig.1). However, these rocks are more probably related to the second extensional event.

The Western Sierras Pampeanas Grenvillian basement has been correlated with other outcrops of Proterozoic basement in South America, i.e., the Arequipa-Antofalla block and Amazonia, on the basis of geochronology of detrital zircons and Nd and Pb isotope geochemistry (Casquet et al., 2006, 2008b). It is probable that these continental masses were accreted to Laurentia through the Grenville-Sunsás orogeny between 1.2 and 1.05 Ga and thus amalgamated to the Rodinia supercontinent, with Laurentia in a central position. The process involved a still highly conjectural history of collision and further protracted lateral displacement of Amazonia along the boundary between the two continents (e.g., Loewy et al., 2003, 2004; Tohver et al., 2002, 2004; Boger et al., 2005; Cordani and Teixeira, 2007, among others). In the Neoproterozoic and Early Paleozoic, the continental masses mentioned above, i.e., Laurentia, Amazonia, Western Sierras Pampeanas, Arequipa-Antofalla and other minor cratons such as Rio Apa (Cordani et al., 2008) remained attached, forming a large continent that was involved in the Pampean orogeny between 535 and 520 Ma (Casquet et al., 2008c). This orogeny resulted from collision with other Gondwanan cratons to the east (present coordinates), probably Kalahari, and led to closure of the intervening Clymene Ocean (Trindade et al., 2006) and the final amalgamation of SW Gondwana (Rapela et al., 2007).

A-type orthogneisses in the Western Sierras Pampeanas are thus a record of Rodinia break-up that took place through a sequence of events in the Neoproterozoic. Allegedly mantle-plume related break-up pulses that affected large areas of the Earth have been recognized in different continents at ca. 825, 780 and 750 Ma (Li et al., 2008). The age reported by Baldo et al. (2006) (ca. 774 Ma) matches well one of the pulses mentioned above, whereas the age of the metagranitoids reported in this contribution is the oldest yet. In the case of the Western Sierras Pampeanas Grenvillian basement these events resulted only in aborted rifts, inasmuch as no evidence for oceanic crust of Neoproterozoic age has been reported so far. Of relevance to our case is the opening of the Iapetus Ocean between Laurentia and Amazonia that took place near the Neoproterozoic-to-Cambrian transition after a long rifting initiated as early as 765 Ma (Tollo et al., 2004). Drifting apart from Laurentia led to development of passive margin sedimentary sequences on both sides of the Iapetus Ocean almost coeval with the Pampean collision (Casquet et al., 2008b). A record of this process is represented by

the Argentine Precordillera carbonate platform, located west of the Sierras Pampeanas (e.g., Astini et al., 1995). Regardless of whether this platform is an exotic terrane travelled from the western margin of the Iapetus and accreted to western Gondwana in the early Paleozoic (reviews in Thomas and Astini, 2003; Ramos, 2004) or a para-autochthonous terrane (e.g., Finney, 2007; Casquet et al., 2008c), it provides evidence that the Western Sierras Pampeanas Grenvillian basement was also part of the drifted conjugate margin of Iapetus.

From the above discussion we infer that break-up of Rodinia along the Grenvillian boundary between Amazonia (+ Western Sierras Pampeanas + Arequipa-Antofalla) and Laurentia was protracted, starting at least at ca. 845 Ma and ending through drifting and ocean opening in the early Cambrian.

A few examples of A-type granitoids from elsewhere in South America coeval with those described here were recognized by Basei et al. (2008) in the reworked basement of the Brasiliano – Panafricano Dom Feliciano Belt , southern Brazil. Ages of 835 ± 9 MA (IDTIMS) and 843 ± 12 Ma (SHRIMP) were obtained that are within error of those found here. Whether this rifting event in southern Brazil was spatially connected through the continental hinterland with that in the Western Sierras Pampeanas, or alternatively records coeval but independent extensional processes in a separate craton (such as the Rio de la Plata craton, Kröner and Cordani, 2003; Fig.3), remains conjectural. Recent geochronological, paleomagnetic and geological evidence for southern South American cratons in the Neoproterozoic (Rapela et al., 2007) seem to favour the second interpretation.

It is notable that the rifting event at ca. 845 Ma was almost coeval with consumption of the Brasiliano Ocean between the São Francisco/Congo and the Amazonia and Paraná cratons in the early Neoproterozoic (Kröner and Cordani, 2003). An intra-oceanic magmatic arc, the juvenile Goiás magmatic arc in Central Brazil, existed between ca. 890 and 800 Ma (Pimentel et al., 2000; Laux et al., 2005). Complete consumption of the Brasiliano Ocean took probably place at ca. 600 Ma (Laux et al., 2005). This evidence of subduction in the early Neoproterozoic has been taken as a proof that some large cratons such as São Francisco/Congo and others were not part of the Rodinia supercontinent (Cordani et al., 2003; Kröner and Cordani, 2003). We can only state that the rifting events at ca. 845 Ma and ca. 774 Ma were comparatively very short and took place while subduction of the Brasiliano Ocean was underway.

The age of the metamorphic rims in zircon grains from ESP-7066 (ca. 420 Ma, i.e., Silurian) confirms that a strong metamorphic overprint took place during the Ordovician–Silurian Famatinian orogeny. Although still poorly known in detail (time and P-T conditions) the Famatinian overprint in the sierras of Maz and Espinal was widespread, varying from greenschist to upper garnet-amphibolite facies conditions (Lucassen and Becchio, 2003; Casquet et al., 2008 b). Because no conclusive evidence exists in the sierras of Maz and Espinal of orogeny between ca. 840 Ma and the Famatinian orogeny (however, see Mulcahy et al., 2007 and Casquet et al., 2008c), high-grade metamorphism (664 ± 70ºC) at the site of MAZ-6037 was probably Famatinian. The thin low-U zircon rims in sample MAZ-6037 were unfortunately undatable. Since sample ESP-7066 underwent metamorphism at much lower grade than MAZ-6037, it is suggested that zircon overgrowths in this case might be related to the pervasive influx of fluids leading to retrogression of the igneous association. Zircon

crystallization seems possible from aqueous fluids under low P and T conditions (< 500ºC) and high water/rock ratios (Corfu et al., 2003, Dempster et al. 2004, Rasmussen 2005).

Acknowledgements

This work is a contribution to the Argentine projects CONICET PIP 5719, FONCYT PICT 1728/OC AR and the Spanis CGL2005-02065/BTE (MEC) and 910495 (2007) (UCM). R.J. Pankhurst acknowledges a Small Research Grant from NERC (Great Britain). F. Colombo thanks CONICET for a travel grant to do analytical work. We are very grateful to Profs Umberto Cordani and Randy Parrish and an anonymous reviewer for their insightful and constructive criticisms that greatly improved the manuscript.

References

Astini, R.A., Benedetto, J.L., Vaccari, N.E., 1995. The early Paleozoic evolution of the Argentina Precordillera as a Laurentian rifted, drifted and collided terrane: a geodynamic model. Geological Society American Bulletin 107, 253-273.

Baldo, E.G., Casquet, C., Pankhurst, R.J., Galindo, C., Rapela, C.W., Fanning, M., Dahlquist, J.A., Murra, J., 2006. Neoproterozoic A-type granitic magmatism in the Western Sierras Pampeanas (Argentina): evidence for Rodinia break-up along a proto-Iapetus rift?. Terra Nova 18, 388–394.

Basei, M.A.S., Grasso, C.B., Vlach, S.R.F., Nutman, A., Siga Jr., O., Osako, L.S., 2008. "A"-type rift-related granite and the Lower Cryogenian age for the beginning of the Brusque Belt Basin, Dom Feliciano Belt, Southern Brazil. VI South American Symposium on Isotope Geology. Proceedings in CD. San Carlos de Bariloche.

Boger, S.D., Raetz, M., Giles, D., Etchart, E., Fanning, C.M., 2005. U-Pb data from the Sunsas region of Eastern Bolivia, evidence for an allochthonous origin of the Paragua block. Precambrian Research 139, 121-146.

Bonin, B., 2007. A-type granites and related rocks: Evolution of a concept, problems and prospects. Lithos 97, 1-29.

Boyton, W.V., 1984. Cosmochemistry of the rare earth elements: meteorite studies. In: Henderson, P. (Ed.). Rare earth element geochemistry. Elsevier. 63-114. Amsterdam.

Casquet, C., Rapela, C.W., Pankhurst, R.J., Fanning, M., Baldo, E., González-Casado, J.M., Galindo, C., Dahlquist, J.A., 2006. U-Pb SHRIMP zircon dating of Grenvillian metamorphism in Western Sierras Pampeanas (Argentina): correlation with the Arequipa–Antofalla craton and constraints on the extent of the Precordillera Terrane. Gondwana Research Letter 9, 524-529.

Casquet, C., Rapela, C.W., Pankhurst, R.J., Galindo, C., Dahlquist , J., Baldo, E.G., Saavedra, J.M., González-Casado, J.M., Fanning, M., 2005. Grenvillian massif-type anorthosites in the Sierras Pampeanas. Journal of the Geological Society, (London) 162, 9-12.

Casquet, C., Rapela, C.W., Baldo, E., Pankhurst, R.J., Dahlquist, J., González-Casado, J.M., Galindo, C., Fanning, C.M., Saavedra, J., 2008a. Allochthoneity of the Argentine Precordillera terrane: An alternative to current paleogeographical models. 33th International Geological Congress, Oslo. Proceedings in CD, 1page.

Casquet, C., Pankhurst, R.J., Rapela, C.W., Galindo, C., Fanning, C.M., Chiaradia, M., Baldo, E.G., González Casado, J.M., Dahlquist, J.A., 2008 b. The Mesoproterozoic Maz terrane in the Western Sierras Pampeanas, Argentina, equivalent to the

Arequipa-Antofalla block of southern Peru? Implications for West Gondwana margin evolution. Gondwana Research 13: 163-175.

Casquet, C., Pankhurst, R.J., Galindo, C., Rapela, C.W., Fanning, C.M., Baldo, E.G., Dahlquist, J.A., González Casado, J.M., Colombo, F., 2008 c. A deformed alkaline igneous rock – carbonatite complex from the Western Sierras Pampeanas, Argentina: evidence for late Neoproterozoic opening of the Clymene Ocean?. Precambrian Research 165: 205-220.

Cordani, U.G., Brito-Neves, B.B., D'Agrella-Filho, M., 2003. From Rodinia to Gondwana: A Review of the Available Evidence from South America. Gondwana Research 6: 275-283

Cordani, U.G., Tassinari, C.C.G., Teixeira, W., Coutinho, J.M.V., 2008. U-Pb SHRIMP zircon ages for the Rio Apa cratonic fragment in Mato Grosso do Sul (Brazil) and northern Paraguay: Tectonic implications. VI South American Symposium on Isotope Geology, Bariloche, Argentina. Proceedings in CD.

Cordani, U.G., Teixeira, W., 2007. Proterozoic accretionary belts in the Amazonian Craton. In: Hatcher, R.D. Jr., Carlson, M.P., McBride, J.H., Martínez Catalán, J.R. (Eds.). 4-D Framework of Continental Crust. Geological Society of America, Memoir 200, 297-320.

Corfu, F., Hanchar, J.M., Hoskin, P.W.O., Kinny, P., 2003. Atlas of Zircon Textures. In: Hanchar, J. M. and Hoskin, P. W. O. (Eds.) Zircon. Reviews in Mineralogy and Geochemistry 53: 469-500. Mineralogical Society of America and Geochemical Society. Washington, D.C.

Dahlquist, J.A., Galindo, C., Pankhurst, R.J., Rapela, C.W., Alasino, P.H., Saavedra, J., Fanning, C.M., 2007. Magmatic evolution of the Peñón Rosado granite: petrogenesis of garnet-bearing granitoids. Lithos 95, 177-207.

Dalziel, I.W.D. 1991. Pacific margins of Laurentia and East Antarctica-Australia as a conjugate rift pair; evidence and implications for an Eocambrian supercontinent Geology (Boulder) 19(6), 598-601.

De Paolo, D.J., Perry, F.V., Baldridge, W.S., 1992. Crustal versus mantle sources of granitic magmas: a two-parameter model based on Nd isotopic studies. Earth Science Transactions of the Royal Society of Edinburgh 83, 439–446.

Dempster, T.J., Hay, D.C., Bluck, B.J., 2004. Zircon growth in slate. Geology, 32(3), 221-224.

Droop, G. T. R. 1987. A general equation for estimating Fe3+ concentrations in ferromagnesian silicates and oxides from microprobe analyses, using stoichiometric criteria. Mineralogical Magazine 51: 431-435.

Eby, G.N. 1990. The A-type granitoids: A review of their occurrence and chemical characteristics and speculations on their petrogenesis. Lithos 26, 115-134.

Eby, G.N. 1992. Chemical subdivision of the A-type granitoids: Petrogenetic and tectonic implications. Geology, 20, 641-644.

Ercit, T. S. 2002. The mess that is “allanite”. The Canadian Mineralogist 40, 1411-1419.

Finney, S.C., 2007. The parautochthonous Gondwanan origin of the Cuyania (greater Precordillera) terrane of Argentina: A re-evaluation of evidence used to support and allocthonous Laurentian origin. Geologica Acta, 5, 127-158.

Galindo, C., Casquet, C., Baldo, E.G., Pankhurst, R., Rapela, C.W., Saavedra, J., 2004. Sr, C and O Isotope Geochemistry of Carbonates from Sierra de Pie de Palo and other Western Sierras Pampeanas (Argentina). Stratigraphy and Constraints on the Derivation of the Precordillera Terrane. Precambrian Research 131, 57-71.

Harris, N.B.W., Pearce, J.A., Tindle, A.G., 1986. Geochemical characteristics of collision-zone magmatism. In: Coward, M.P., Reis, A.C. (Eds.) Collision Tectonics. Special Publication of the Geological Society 19, 67-81.

Hoffman, P.F., 1991. Did the breakout of Laurentia turn Gondwanaland inside out? Science 252, 1409–1412.

International Comission on Stratigraphy, 2008. International Stratigraphic Chart. http://www.stratigraphy.org/

Jordan T.E., Allmendinger, R.W., 1986. The Sierras Pampeanas of Argentina: a modern analogue of Laramide orogeny. American Journal of Science 286, 737-764.

Kilmuray, J.O., Dalla Salda, L. 1971. Las fases de deformación y metamorfismo en la Sierra de Maz, provincia de La Rioja, República Argentina. Revista de la Asociación Geológica Argentina 26 (2), 245–263.

Kotopouli, C.N., Pe-Piper, G., Piper, D.J.W., 2000. Petrology and evolution of the Hercynian Pieria granitoid complex (Thessaly, Greece); paleogeographic and geodynamic implications. Lithos 50(1-3), 137-152.

Kröner, A., Cordani, U., 2003. African, southern India and South American cratons were not part of the Rodinia supercontinent: evidence from field relationships and geochronology. Tectonophysics 375, 325-352.

Laux, J.H., Pimentel, M.M., Dantas, E.L., Armstrong, R., Junges, S.L., 2005. The Neoproterozoic crustal accretion events in the Brasília belt, central Brazil. Journal of South American Earth Sciences 18, 183-198.

Le Goff, E., Ballevre, M., 1990. Geothermobarometry in albite-garnet orthogneiss; a case study from the Gran Paradiso Nappe (Western Alps). Lithos 25(4), 261-280.

Leake, B.E., Wooley, A.R., Arps, C.E.S., Birch, W.D., Gilbert, M.C., Grice, J.D., Hawthorne, F.C., Kato, A., Kisch, H.J., Krivovichev, V.G., Linthout, K., Laird, J., Mandarino, J., Maresch, W.V., Nickel, E.H., Rock, N.M.S., Schumacher, J. C., Smith, D.C., Stephenson, N.C.N., Ungaretti, L., Whittaker, E.J.W., Youzhi, G., 1997. Nomenclature of amphiboles: Report of the Subcommittee on Amphiboles of the International Mineralogical Association, Commission on New Minerals and Mineral Names. American Mineralogist 82, 1019-1037.

Li, Z. X., Bogdanova, S. V., Collins, A. S., Davidson, A., De Waele, B., Ernst, R. E., Fitzsimons, I. C. W., Fuck, R. A., Gladkochub, D. P., Jacobs, J., Karlstrom, K. E., Lu, S., Natapov, L. M., Pease, V., Pisarevsky, S. A., Thrane, K. y Vernikovsky, V. 2008. Assembly, configuration, and break-up history of Rodinia: A synthesis. Precambrian Research 160, 179-210.

Loewy, S.L., Connelly, J.N., Dalziel, I.W.D., Gower, C.F., 2003. Eastern Laurentia in Rodinia: constraints from whole-rock Pb and U/Pb geochronology. Tectonophysics 375, 169-197.

Loewy, S.L., Connelly, J.N., Dalziel, I.W.D., 2004: An orphaned block: the Arequipa-Antofalla basement of the central Andean margin of South America. GSA Bulletin, 116, 171-187.

Lucassen, F., Becchio, R. 2003. Timing of high-grade metamorphism: Early Palaeozoic U-Pb formation ages of titanite indicate long-standing high-T conditions at the western margin of Gondwana (Argentina, 26-29ºS). Journal of Metamorphic Geology 21, 649-662.

Ludwig K.R. 2001. SQUID 1.02, a User's Manual; Berkeley Geochronology Center Special Publication. No. 2, 2455 Ridge Road, Berkeley, CA 94709, USA.

Ludwig, K.R. 2003. User's manual for Isoplot/Ex, Version 3.0, A geochronological toolkit for Microsoft Excel. Berkeley Geochronology Center Special Publication No. 4, 2455 Ridge Road, Berkeley CA 94709, USA.

McDonough, M., Ramos, V.A., Isachsen, C., Bowring, S. 1993. Edades preliminares de circones del basamento de la Sierra de Pie de Palo, Sierras Pampeanas Occidentales de San Juan: sus implicancias para el supercontinente proterozoico de Rodinia. XVII Congreso Geológico Argentino and II Congreso de Exploración de Hidrocarburos, Proceedings III, 340-343. Mendoza.

Moores, E.M., 1991. Southwest U.S.-East Antarctic (SWEAT) connection; a hypothesis. Geology (Boulder) 19(5), 425-428.

Mulcahy, S.R., McClelland, W.C., Roeske, S.M., Vujovich, G.I., Cain, J.C., 2003. U-Pb zircon analysis from the western Sierras Pampeanas, northwest Argentina; evidence for a complex Proterozoic through Silurian tectonic history. Abstracts with Programs - Geological Society of America 35(6), 344.

Mulcahy, S.R., Roeske, S.M., McCleland, W.C., Nomade, S., Renne, P.R., 2007. Cambrian initiation of the Las Pirquitas thrust on the western Sierras Pampeanas, Argentina: implications for the tectonic evolution of the proto-Andean margin of South America. Geology 35, 443–446.

Paces, J.B., Miller, J.D., 1993. Precise U-Pb ages of Duluth Complex and related mafic intrusions, northeastern Minnesota: Geochronological insights to physical, petrogenetic, paleomagnetic, and tectonomagmatic process associated with the 1.1 Ga Midcontinent Rift System. Journal of Geophysical Research 98(13), 13997-14013.

Pearce, J.A., Harris, N.B.W., Tindle, A.G., 1984. Trace element discrimination diagrams for the tectonic interpretation of granitic rocks. Journal of Petrology 25, 956–983

Pimentel, M.M., Fuck, R.A., Lima Gioia, S.M.C., 2000. The Neoproterozoic Goiás magmatic arc, central Brazil: a review and new Sm-Nd isotopic data. Revista Brasileira de Geociências 30, 35-39.

Porcher, C.C., Fernandes, L.AD., Vujovich, G.I., Chernicoff, C.J., 2004. Thermobarometry, Sm/Nd ages and geophysical evidence for the location of the suture zone between Cuyania and the western proto-Andean margin of Gondwana. Gondwana Research 7(4), 1057-1076.

Powell, R., Holland, T.J.B., 1988. An internally consistent thermodynamic dataset with uncertainties and correlations: 3: application methods, worked examples and a computer program. Journal of Metamorphic Geology 6, 173–204.

Ramos, V.A. 2004. Cuyania, an exotic block to Gondwana: Review of historical success and present problems. Gondwana Research 7, 1009-1026.

Rapela, C.W. , Pankhurst, R.J., Casquet, C., Fanning, C.M., Baldo, E.G., González-Casado,J.M., Galindo, C., Dahlquist, J., 2007. The Río de la Plata craton and the assembly of SW Gondwana. Earth Science Reviews 8, 49-82.

Rapela, C.W., Pankhurst, R.J., Casquet, C., Fanning, C.M., Galindo, C., Baldo, E.G., 2005. Datación U-Pb SHRIMP de circones detríticos en paranfibolitas neoproterozoicas de las secuencia Difunta Correa (Sierras Pampeanas Occidentales, Argentina). Geogaceta 38, 3-6.

Rasmussen, B., 2005. Zircon growth in very low grade metasedimentary rocks: evidence for zirconium mobility at ~250ºC. Contributions to Mineralogy and Petrology 150, 146-155.

Thomas, W.A., Astini, R.A., 2003. Ordovician accretion of the Argentine Precordillera terrane to Gondwana: a review. Journal of South American Earth Sciences 16, 67-79.

Tohver, E., van der Pluijm, B.A., Van der Voo, R., Rizzotto, G., Scandolara, J.E., 2002. Paleogeography of the Amazon craton at 1.2 Ga: Early Grenvillian collision with the Llano segment of Laurentia. Earth and Planatary Science Letters 199, 185-200.

Tohver, E., Bettencourt, J.S., Tosdal, R., Mezger, K., Leite, W.B. and Payolla, B.L., 2004. Terrane transfer during Grenville orogeny: tracing the Amazonian ancestry of southern Appalachian basement through Pb and Nd isotopes. Earth and Planetary Science Letters, 228, 161-176.

Tollo, P.R., Aleinikoff, J.N., Bartholomew, M.J., Rankin, D.W., 2004. Neoproterozoic A-type granitoids of the central and southern Appalachians: intraplate magmatism associated with episodic rifting of the Rodinian supercontinent. Precambrian Research 128, 3-38.

Trindade, R.I.F., D'Agrella-Filho, M.S., Epof, I., Brito Neves, B.B., 2006. Paleomagnetism of Early Cambrian Itbaiana mafic dikes (NE Brazil) and the final assembly of Gondwana. Earth and Planetary Science Letters 244, 361-377.

Varela, R., Valencio, S., Ramos, A., Sato, K., González, P., Panarello, H., Roverano, D., 2001. Isotopic strontium, carbon and oxygen study on Neoproterozoic marbles from Sierra de Umango, Andean foreland, Argentina. III South American Symposium on Isotope Geology. Sociedad Geológica de Chile. CD: 450-453.

Vujovich, G.I., Porcher, C.C., Chernicoff, C.J., Fernandes, L.A.D., Pérez, D.J., 2005. Extremo norte del basamento del terreno Cuyania: nuevos aportes multidisciplinarios para su identificación. Asociación Geológica Argentina, Serie D, Publicación Especial 8, 15-38.

Whalen, J. B., Currie, K.L., Chappell, B.W., 1987. A-type granites; geochemical characteristics, discrimination and petrogenesis. Contributions to Mineralogy and Petrology 95(4), 407-419

Williams, I.S., 1998. U–Th–Pb geochronology by ion microprobe. In: McKibben, M.A., Shanks, W.C. (Eds.), Applications of Microanalytical Techniques to Understanding Mineralising Processes. Reviews in Economic Geology 7, 1–35.

Winchester, J.A., Floyd, P.A., 1977. Geochemical discrimination of different magma series and their differentiation products using immobile elements. Chemical Geology 20, 325-343.

Table 1

	ESP-7066	MAZ-12040
wt. %		
SiO_2	77.50	68.84
Al_2O_3	7.90	13.60
$Fe_2O_3^*$	4.20	6.35
MnO	0.04	0.09
MgO	0.98	0.23
CaO	0.98	2.19
Na_2O	0.58	2.92
K_2O	4.85	4.73
TiO_2	1.17	0.56
P_2O_5	0.09	0.17
LOI	1.42	0.58
Total	99.68	100.30
ppm		
Sc	6	9
Be	<1	2
V	43	7
Cr	48	40
Co	6	3
Ni	<20	<20
Cu	<10	20
Zn	49	120
Ga	10	28
Ge	1.2	1.4
Rb	54	74
Sr	97	232
Y	43.7	75.9
Zr	603	891
Nb	23.6	27.5
Mo	<2	3
Cs	0.4	0.5
Ba	1051	1787
Hf	14.7	21.3
Ta	2.26	1.56
W	1.3	<0.5
Tl	0.33	0.33
Pb	17	14
Bi	<0.1	<0.1
Th	15.5	1.77
U	1.88	0.65
La	81.79	40.70
Ce	180.05	97.10
Pr	16.39	13.60
Nd	63.71	60.40
Sm	11.65	14.30
Eu	2.15	5.17
Gd	8.97	14.70
Tb	1.45	2.52
Dy	8.21	14.80
Ho	1.61	2.88
Er	4.64	8.38
Tm	0.72	1.20
Yb	4.50	7.59
Lu	0.67	1.19

<x: below the detection limit (x)

Table 2

sample	Sm	Nd	Sm/Nd	$^{147}Sm/^{144}Nd$	$^{143}Nd/^{144}Nd$	$^{143}Nd/^{144}Nd_i$	εNd_i	TDM	2TDM	Rb	Sr	Rb/Sr	$^{87}Rb/^{86}Sr$	$^{87}Sr/^{86}Sr$	$^{87}Sr/^{86}Sr_i$	εSr_i
MAZ-12040	14.3	60.4	0.2368	0.1431	0.512358	0.511564	+0.3	1459	1446	74	232	0.3190	0.9238	0.717962	0.706810	+47
ESP-7066	11.7	63.7	0.1837	0.1110	0.512084	0.511469	-1.5	1413	1595	54	97	0.5567	1.6136	0.726144	0.706666	+45

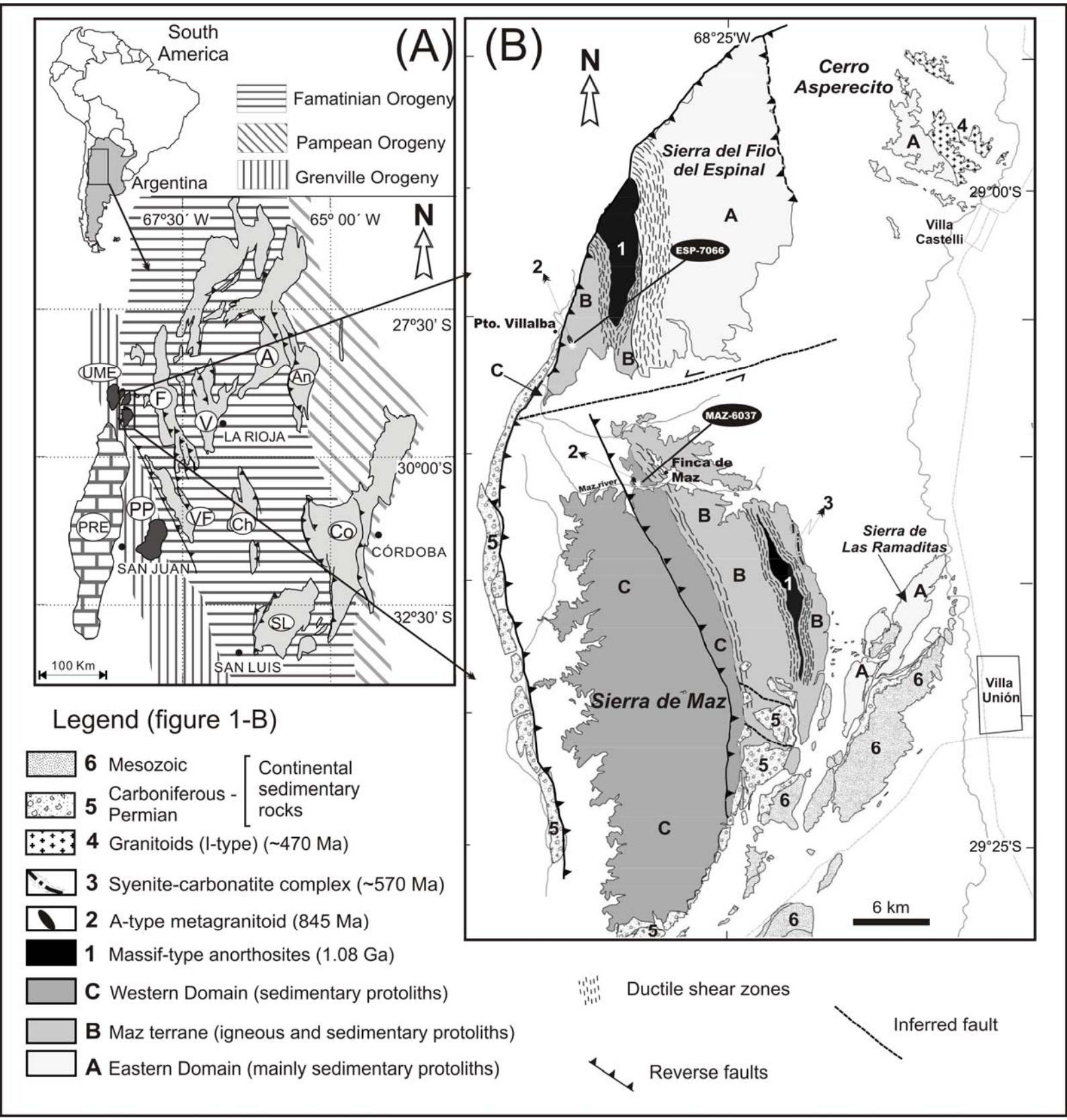
(A)
South America
Argentina
Famatinian Orogeny
Pampean Orogeny
Grenville Orogeny
67°30´ W
65° 00´ W
N
27°30' S
30°00'S
32°30' S
100 Km
UME
F
V
A
An
LA RIOJA
PP
PRE
VF
Ch
Co
SAN JUAN
CÓRDOBA
SL
SAN LUIS
(B)
68°25'W
N
Cerro Asperecito
Sierra del Filo del Espinal
ESP-7066
Pto. Villalba
MAZ-6037
Finca de Maz
Maz river
Sierra de Las Ramaditas
Sierra de Maz
Villa Castelli
Villa Unión
29°00'S
29°25'S
6 km
Legend (figure 1-B)
6 Mesozoic
5 Carboniferous - Permian
Continental sedimentary rocks
4 Granitoids (I-type) (~470 Ma)
3 Syenite-carbonatite complex (~570 Ma)
2 A-type metagranitoid (845 Ma)
1 Massif-type anorthosites (1.08 Ga)
C Western Domain (sedimentary protoliths)
B Maz terrane (igneous and sedimentary protoliths)
A Eastern Domain (mainly sedimentary protoliths)
Ductile shear zones
Inferred fault
Reverse faults

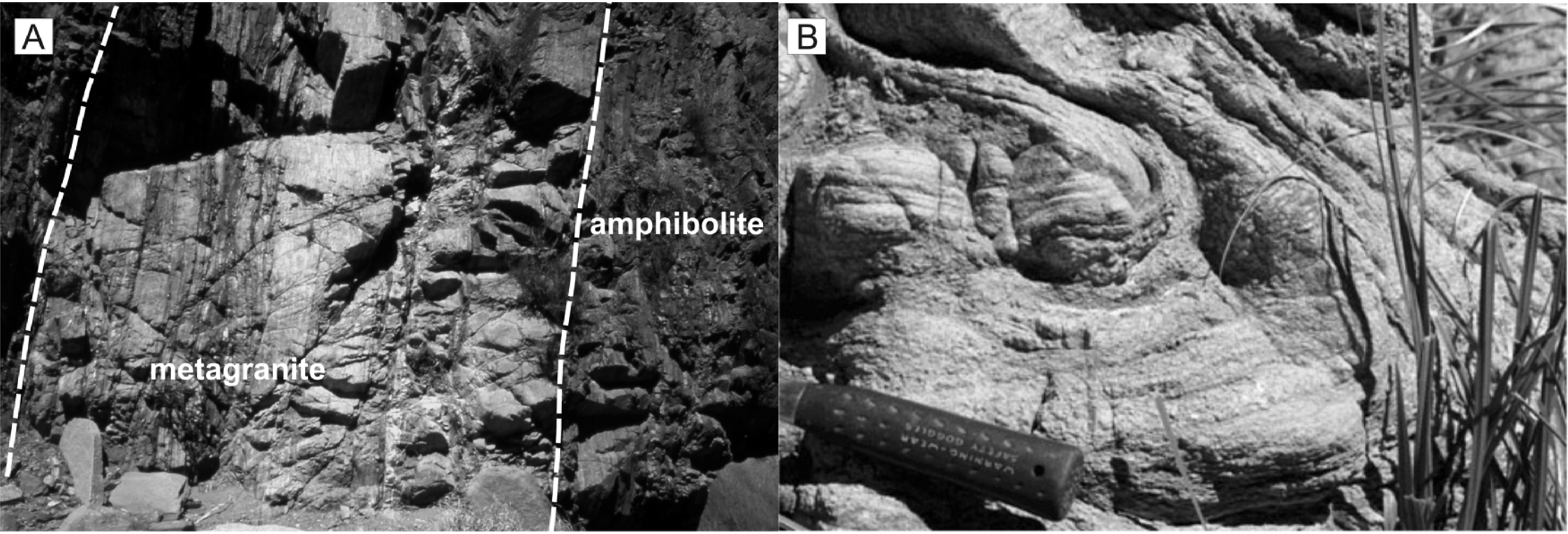
A
amphibolite
metagranite
B

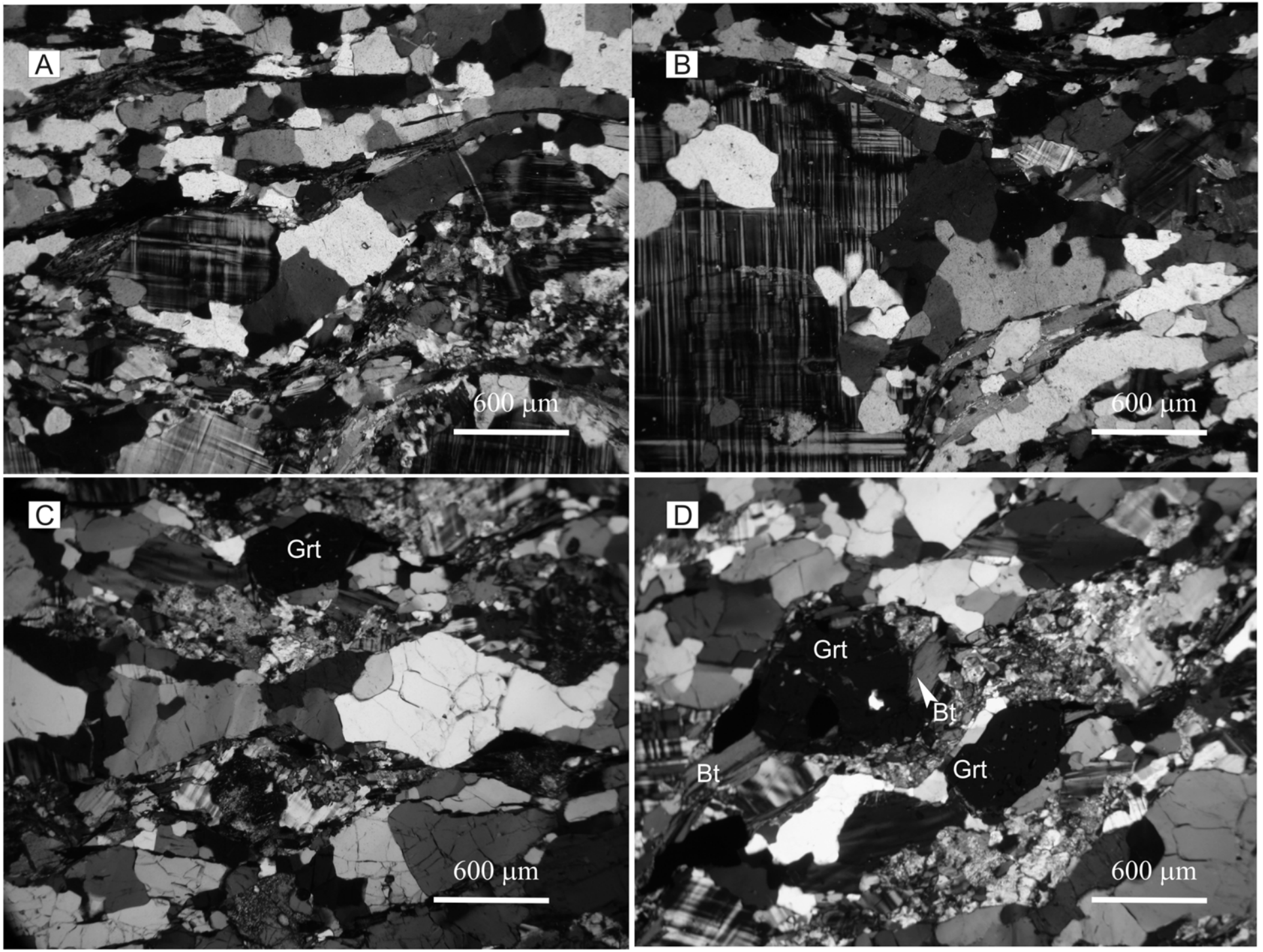
A
600 μm
B
600 μm
C
Grt
600 μm
D
Grt
Bt
Bt
Grt
600 μm

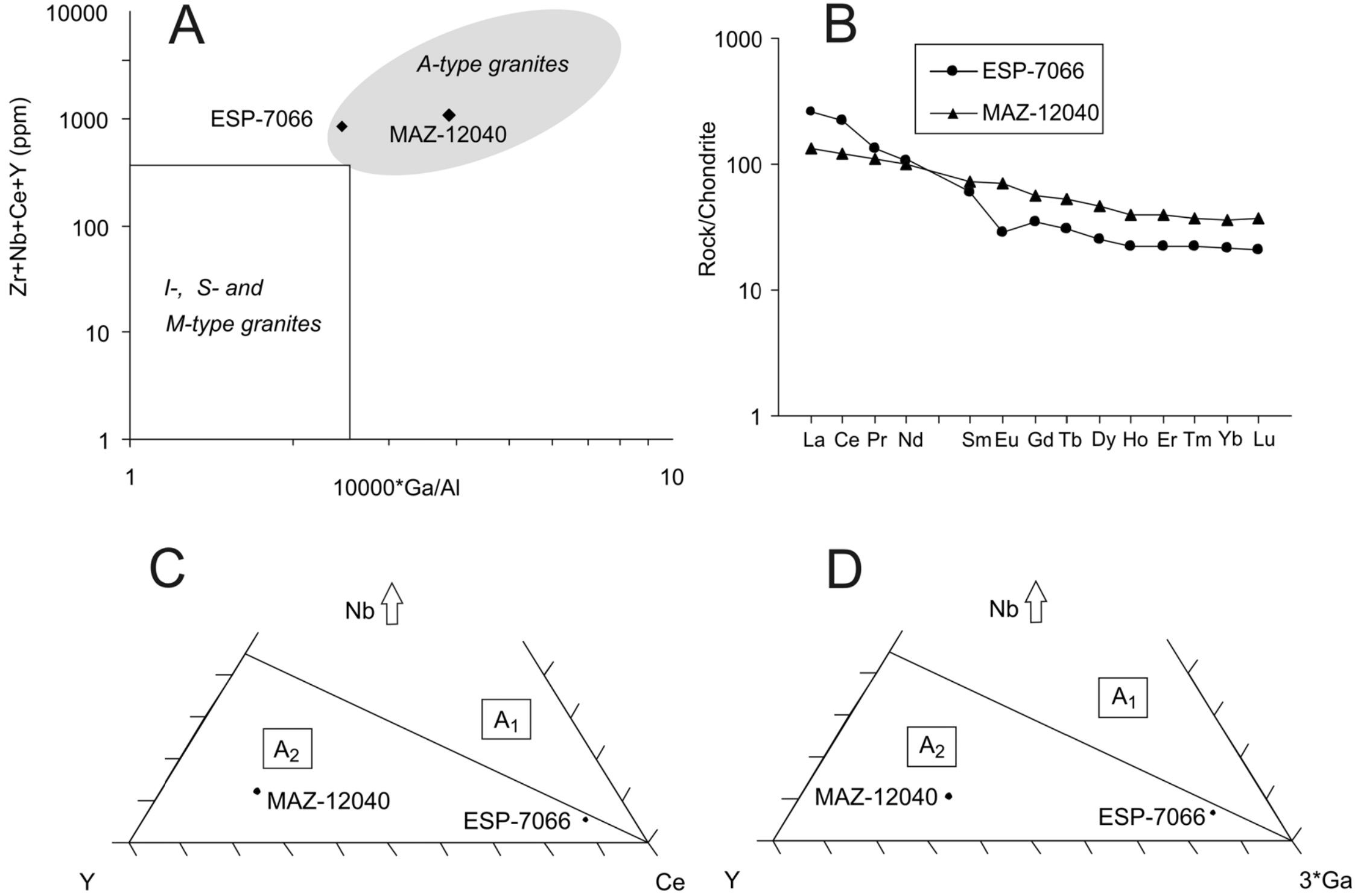
A
10000
1000
100
10
1
Zr+Nb+Ce+Y (ppm)
A-type granites
ESP-7066
MAZ-12040
I-, S- and
M-type granites
1
10000*Ga/Al
10
B
1000
100
10
1
Rock/Chondrite
ESP-7066
MAZ-12040
La Ce Pr Nd Sm Eu Gd Tb Dy Ho Er Tm Yb Lu
C
Nb
A2
A1
MAZ-12040
ESP-7066
Y
Ce
D
Nb
A1
A2
MAZ-12040
ESP-7066
Y
3*Ga


A
825
843
877
871
857
864
833
500µm
MAZ-6037

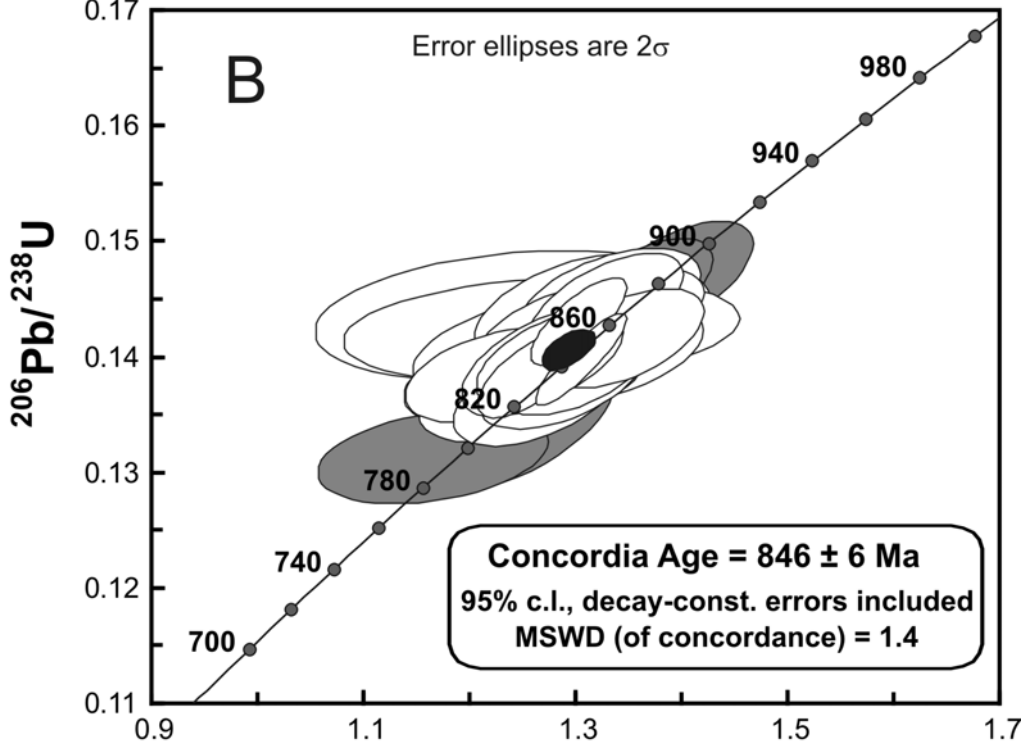
B
Error ellipses are 2σ
980
940
900
860
820
780
740
700
Concordia Age = 846 ± 6 Ma
95% c.l., decay-const. errors included
MSWD (of concordance) = 1.4
206Pb/238U
0.17
0.16
0.15
0.14
0.13
0.12
0.11
0.9
1.1
1.3
1.5
1.7

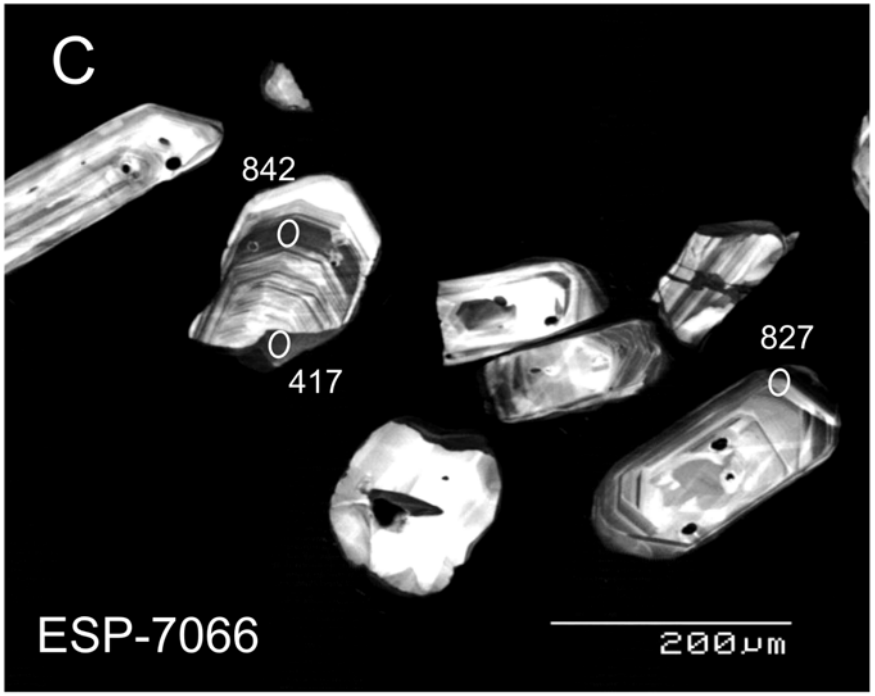
C
842
417
827
200µm
ESP-7066

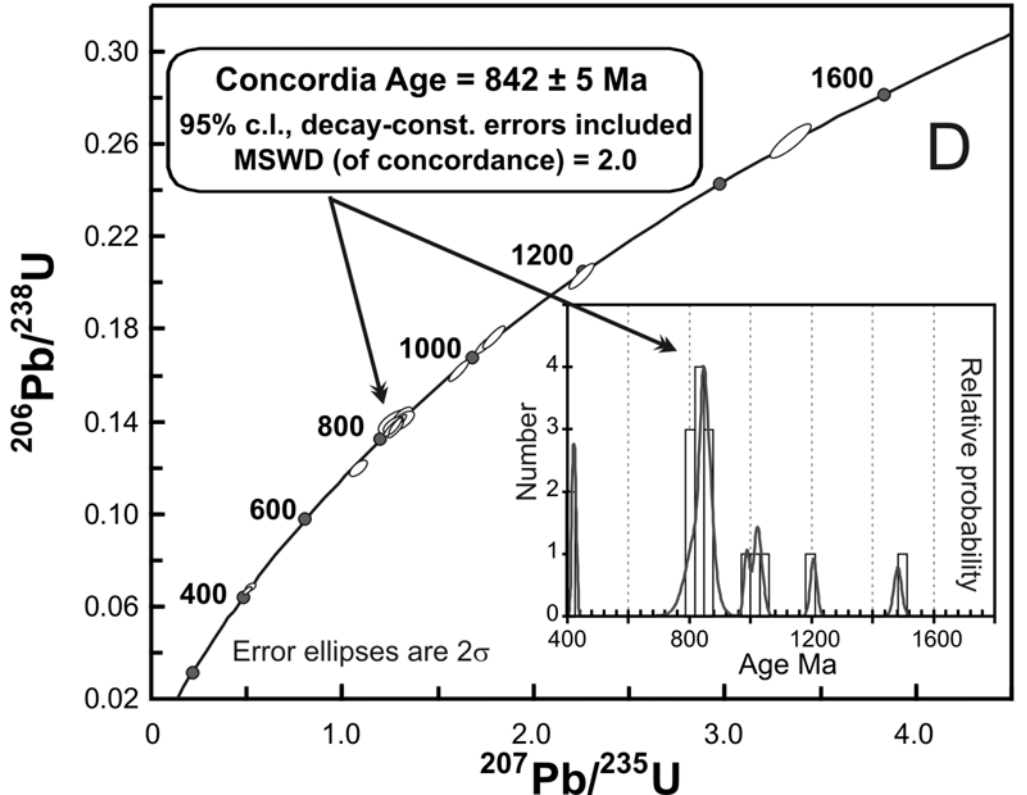
D
Concordia Age = 842 ± 5 Ma
95% c.l., decay-const. errors included
MSWD (of concordance) = 2.0
1600
1200
1000
800
600
400
Error ellipses are 2σ
Number
Relative probability
Age Ma
400
800
1200
1600
206Pb/238U
0.30
0.26
0.22
0.18
0.14
0.10
0.06
0.02
0
1.0
2.0
3.0
4.0
207Pb/235U

Electron microprobe analyses

Analyses were performed with a JEOL JXA 8900M microprobe using with 15 kV, 20 nA (20 kV and 150 nA for epidote) and a beam diameter of 5 μm. An element was considered to be present if its concentration exceeded twice the calculated detection limit.

Standards included albite (Si, Na), sillimanite (Al), almandine (Fe and Mn), kaersutite (Mg, Ca and Ti), potassium feldspar (K), fluorapatite (F, Cl, P), zircon (Hf, Zr), and synthetic compounds (U, Th, REE, Y, Ni, Cr).

Selected electron microprobe analyses of minerals from sample MAZ-6037

Wt. %	Microcline	Plagioclase		Biotite	Titanite		Amphibole	Garnet	
	#6	#5	#29	#22	#47	#52	#41	#16	#11
SiO_2	63.87	61.65	65.90	33.27	29.83	29.44	37.45	37.69	37.63
TiO_2	<0.08	<0.08	<0.08	2.68	36.51	35.51	1.45	0.06	0.21
Al_2O_3	18.65	23.81	21.51	16.58	1.73	2.07	13.57	20.65	20.42
Fe_2O_3	<0.09	<0.09	0.20		1.00	1.52	2.71	17.27	16.70
FeO				31.21			25.67	9.21	11.09
MnO	<0.08	<0.08	<0.08	0.35	0.09	0.05	0.27	6.09	4.73
MgO	<0.04	<0.04	<0.04	2.24	<0.05	<0.05	2.17	0.28	0.47
CaO	<0.04	5.28	3.06	<0.04	29.78	28.88	11.33	11.57	11.02
ZnO				0.26	<0.16	<0.16	0.00	<0.14	<0.14
Y_2O_3					0.21	1.61	<0.05		
Na_2O	0.55	8.51	9.75	<0.03	<0.03	0.04	1.43	<0.03	<0.03
K_2O	16.16	0.38	0.07	9.24			2.04		
F				<0.14	0.21	0.26	0.00	<0.14	<0.14
Cl				0.03	0.06	<0.02	0.06		
H_2O_{calc}				3.69	0.31	0.41	1.86		
Total	99.23	99.63	100.49	99.53	99.72	99.79	99.99	102.82	102.27
Formula	(apfu)								
Si	2.979	2.747	2.884	2.696	0.971	0.963	5.986	2.993	3.004
Ti	0.000	0.000	0.000	0.164	0.894	0.874	0.174	0.003	0.013
Al	1.025	1.251	1.109	1.584	0.066	0.080	2.557	1.933	1.921
Fe^{3+}	0.000	0.000	0.006		0.025	0.037	0.326	1.032	1.003
Fe^{2+}				2.115			3.431	0.612	0.740
Mn	0.000	0.000	0.000	0.024	0.002	0.001	0.036	0.410	0.319
Mg	0.000	0.000	0.000	0.271	0.000	0.000	0.516	0.034	0.056
Ca	0.000	0.252	0.143	0.000	1.038	1.013	1.941	0.984	0.942
Zn				0.015	0.000	0.000	0.000		
Y				0.000	0.004	0.028		0.000	0.000
Na	0.049	0.735	0.828	0.000	0.000	0.003	0.443		
K	0.961	0.022	0.004	0.955			0.416		
F					0.021	0.027	0.000		
Cl				0.004	0.003	0.000	0.017		
OH_{calc}				1.996	0.066	0.090	1.983		

Plagioclase: #5: core; #29: rim. Titanite: #47: core; #52: rim. Garnet: #16: core; #11: rim. Blank: not measured. <x: less than the stated detection limit (at 2σ). Sought but not found (detection limit in ppm, 2σ): Ni (660), Cr (450). H_2O calculated by stoichiometry. Microcline, plagioclase and titanite: all Fe expressed as Fe_2O_3. Biotite: all Fe expressed as FeO. Amphibole: Fe^{2+}/Fe^{3+} calculated after Leake et al. (1997). Garnet: Fe^{2+}/Fe^{3+} calculated based on 12 O and 8 cations, after Droop (1987). Structural formulae

calculated on the basis of 8 O (microcline and plagioclase), 11 O eq. (biotite), 3 cations (titanite), and 23 O eq. (amphibole).

Electron microprobe analyses of epidote from sample MAZ-6037

Wt. %	#6	#2
SiO_2	33.79	37.40
TiO_2	0.27	0.15
Al_2O_3	21.97	24.31
Fe_2O_3	8.10	11.09
FeO	4.25	1.26
MnO	0.16	0.14
MgO	0.09	0.00
CaO	18.40	24.24
P_2O_5	0.03	
Y_2O_3	1.01	<0.06
La_2O_3	1.58	
Ce_2O_3	3.83	
Pr_2O_3	0.47	
Nd_2O_3	2.18	
Sm_2O_3	0.42	
Gd_2O_3	0.42	
Dy_2O_3	0.26	
Er_2O_3	0.14	
Yb_2O_3	0.11	
Lu_2O_3	0.04	
ThO_2	0.03	
H_2O_{calc}	1.74	1.89
Total	99.31	100.47
Formula	(apfu)	
Si	2.903	2.966
Ti	0.018	0.009
Al	2.225	2.272
Fe^{3+}	0.524	0.662
Fe^{2+}	0.305	0.083
Mn	0.012	0.009
Mg	0.012	0.000
Ca	1.694	2.059
P	0.002	0.000
Y	0.046	0.000
La	0.050	0.000
Ce	0.121	0.000
Pr	0.015	0.000
Nd	0.067	0.000
Sm	0.013	0.000
Gd	0.012	0.000
Dy	0.007	0.000
Er	0.004	0.000
Yb	0.003	0.000
Lu	0.001	0.000
Th	0.001	0.000
OH_{calc}	1.000	1.000

#6: core, #2: rim. H_2O calculated by stoichiometry to give 1 $(OH)^-$. Fe^{2+}/Fe^{3+} calculated according to Ercit (2002). Blank: not measured. <x: less than the stated detection limit (at 2σ). Sought but not found (detection limit in ppm, 2σ):Tb (140), Ho (240), Tm (1200), U (100), Pb (80), Zr (120), Hf (100), F (1200), Cl (220), Cr (480), Na (260), K (260), Zn (1400).

Electron microprobe analyses of minerals from an amphibolite (sample MAZ-12046) used for thermobarometric calculations.

Wt. %	Biotite				Amphibole							
	#125	#130	#142	#151	#124	#126	#128	#132	#133	#137	#141	#154
SiO_2	35.55	35.44	34.95	36.20	40.24	41.52	40.84	40.83	40.80	40.47	40.95	40.44
TiO_2	1.95	2.42	2.16	2.26	0.84	0.68	0.63	0.56	0.74	0.68	0.66	0.59
Al_2O_3	17.18	16.67	17.54	17.44	15.50	15.28	15.26	15.64	15.05	15.52	15.47	16.02
Fe_2O_3					3.33	2.28	2.31	1.87	3.46	0.83	1.83	0.95
FeO	19.26	20.25	23.09	20.34	16.49	17.03	17.00	17.16	16.69	17.22	16.89	18.13
MnO	0.05	0.10	0.09	0.13	0.20	0.17	0.13	0.09	0.20	0.20	0.18	0.17
MgO	10.01	9.85	7.57	9.75	7.37	7.40	7.27	7.13	7.39	7.07	7.29	6.50
CaO	0.18	0.15	0.07	0.11	11.75	11.47	11.72	11.71	11.57	11.85	11.69	11.80
ZnO	0.20	<0.12	<0.12	<0.12	<0.12	<0.12	<0.12	<0.12	<0.12	0.17	<0.12	0.14
Na_2O	0.09	0.14	0.14	0.14	1.75	1.67	1.67	1.66	1.76	1.67	1.64	1.74
K_2O	8.68	8.76	9.30	9.43	0.80	0.61	0.65	0.62	0.67	0.67	0.59	0.65
Cl	0.09	0.09	0.09	0.08	0.05	0.06	0.11	0.08	0.07	0.07	0.08	0.07
$H2O_{calc.}$	3.83	3.84	3.82	3.92	1.98	1.98	1.95	1.96	1.97	1.94	1.96	1.95
Total	97.06	97.70	98.79	99.78	100.29	100.14	99.53	99.32	100.36	98.35	99.22	99.13
Formula	(apfu)											
Si	2.763	2.752	2.725	2.753	6.062	6.228	6.182	6.183	6.137	6.192	6.199	6.160
Ti	0.114	0.142	0.127	0.129	0.096	0.076	0.071	0.064	0.084	0.079	0.075	0.067
Al	1.574	1.526	1.612	1.563	2.752	2.700	2.723	2.792	2.668	2.799	2.760	2.875
Fe^{3+}					0.378	0.258	0.263	0.213	0.392	0.096	0.208	0.109
Fe^{2+}	1.252	1.315	1.506	1.294	2.078	2.136	2.152	2.173	2.100	2.204	2.139	2.310
Mn	0.003	0.007	0.006	0.008	0.025	0.021	0.017	0.011	0.026	0.026	0.022	0.022
Mg	1.160	1.140	0.880	1.106	1.656	1.655	1.639	1.610	1.657	1.612	1.645	1.476
Zn	0.011	0.000	0.000	0.000	0.000	0.000	0.000	0.000	0.000	0.019	0.000	0.016
Ca	0.015	0.013	0.006	0.009	1.897	1.842	1.901	1.900	1.864	1.943	1.896	1.926
Na	0.013	0.021	0.022	0.021	0.510	0.486	0.489	0.487	0.515	0.494	0.482	0.515
K	0.861	0.868	0.925	0.915	0.155	0.116	0.125	0.120	0.128	0.130	0.113	0.126
Cl	0.012	0.011	0.012	0.011	0.011	0.016	0.029	0.021	0.017	0.017	0.021	0.018
OH_{calc}	1.988	1.989	1.988	1.989	1.989	1.984	1.971	1.979	1.983	1.983	1.979	1.982

<x: less than the stated detection limit (at 2σ). H_2O calculated by stoichiometry. Biotite: all Fe expressed as FeO. Amphibole: Fe^{2+}/Fe^{3+} calculated after Leake et al. (1997). Structural formulae calculated on the basis of 11 O eq. (biotite) and 23 O eq. (amphibole).

Wt. %	Garnet								
	#121	#122	#127	#129	#135	#143	#144	#152	#153
SiO_2	38.07	37.76	38.14	38.14	37.84	37.81	37.59	38.04	38.21
TiO_2	0.13	0.14	0.05	0.00	0.00	0.07	0.11	0.14	0.00
Al_2O_3	21.46	21.19	21.62	21.25	21.63	21.72	21.48	21.81	21.39
Fe_2O_3	0.00	0.00	0.00	0.00	0.00	0.00	0.94	0.62	0.30
FeO	29.46	29.02	29.38	29.42	29.10	25.51	27.53	30.94	29.43
MnO	2.12	2.60	2.67	2.40	2.56	2.35	2.46	1.27	1.88
MgO	3.06	2.63	2.69	2.99	2.60	2.63	2.53	3.29	2.96
CaO	6.22	6.55	6.77	6.47	6.75	7.69	7.12	5.74	7.09
Na_2O	<0.03	<0.03	<0.03	<0.03	<0.03	<0.03	0.30	0.03	<0.03
Total	100.52	99.89	101.33	100.66	100.47	97.79	100.06	101.88	101.26
Formula	(apfu)								
Si	3.007	3.009	2.998	3.013	2.997	3.032	2.984	2.972	3.001
Ti	0.008	0.008	0.003	0.000	0.000	0.004	0.006	0.008	0.000
Al	1.998	1.990	2.003	1.979	2.019	2.054	2.010	2.008	1.980
Fe^{3+}	0.000	0.000	0.000	0.000	0.000	0.000	0.056	0.036	0.018
Fe^{2+}	1.946	1.934	1.931	1.944	1.928	1.711	1.827	2.022	1.933
Mn	0.142	0.175	0.178	0.160	0.172	0.160	0.165	0.084	0.125
Mg	0.360	0.312	0.316	0.352	0.307	0.315	0.299	0.383	0.347
Ca	0.526	0.559	0.570	0.548	0.572	0.661	0.606	0.480	0.596
Na	0.000	0.000	0.000	0.000	0.000	0.000	0.046	0.005	0.000

<x: less than the stated detection limit (at 2σ).
Fe^{2+}/Fe^{3+} calculated based on 12 O and 8 cations, after Droop (1987).

Wt. %	Plagioclase				Ilmenite
	#131	#136	#139	#140	#222
SiO_2	57.37	59.89	59.56	57.07	0.10
TiO_2					46.76
Al_2O_3	26.24	24.72	25.11	27.07	1.55
Fe_2O_3	0.09	0.15	0.32	0.04	9.13
FeO					41.46
MnO					0.37
MgO	<0.03	<0.03	<0.03	<0.03	0.08
CaO	8.32	6.89	6.85	9.57	0.17
Na_2O	7.01	7.90	8.02	6.31	
K_2O	0.05	0.04	0.07	0.09	
Total	99.07	99.59	99.92	100.15	99.60
Formula	(apfu)				
Si	2.593	2.681	2.661	2.558	0.002
Ti					0.888
Al	1.398	1.304	1.322	1.430	0.046
Fe^{3+}	0.003	0.005	0.011	0.001	0.173
Fe^{2+}					0.875
Mn					0.008
Mg					0.003
Zn					0.004
Ca	0.403	0.331	0.328	0.460	
Na	0.614	0.685	0.695	0.548	
K	0.003	0.002	0.004	0.005	

Blank: not measured. <x: less than the stated detection limit (at 2σ). Plagioclase: all Fe expressed as Fe_2O_3. Structural formulae calculated on the basis of 8 O (plagioclase) and 2 cations (ilmenite).

SHRIMP U-Pb data for samples MAZ-6037 and ESP-7066.

Grain. spot	Zircon type	U (ppm)	Th (ppm)	Th/U	Pb* (ppm)	$^{204}Pb/^{206}Pb$	f_{206} %	Radiogenic Ratios $^{206}Pb/^{238}U$	±	$^{207}Pb/^{235}U$	±	$^{207}Pb/^{206}Pb$	±	ρ	Age (Ma) $^{206}Pb/^{238}U$	±	$^{207}Pb/^{206}Pb$	±	% Disc
MAZ-6037																			
1,1	weakly zoned outer	100	45	0,45	12,5	0,000263	0,46	0,1447	0,0019	1,330	0,035	0,0667	0,0015	0,500	871	11	829	48	-5
1,2	core	85	60	0,71	10,3	0,000159	0,27	0,1397	0,0019	1,298	0,031	0,0674	0,0013	0,580	843	11	850	40	1
2,1	weakly zoned outer	128	47	0,37	15,8	0,000664	1,16	0,1421	0,0019	1,268	0,077	0,0647	0,0038	0,216	857	10	765	124	-11
3,1	weakly zoned outer	46	24	0,52	5,8	0,000840	1,48	0,1434	0,0023	1,241	0,076	0,0627	0,0037	0,260	864	13	700	126	-19
*4.1	weakly zoned	137	74	0,54	17,2	0,000028	0,05	0,1457	0,0018	1,360	0,028	0,0677	0,0011	0,590	877	10	859	35	-2
7,1	osc.-zoned outer	159	90	0,57	18,9	0,000069	0,12	0,1379	0,0018	1,287	0,032	0,0677	0,0014	0,519	833	10	860	44	3
8,1	osc.-zoned outer	139	50	0,36	16,4	0,000264	0,46	0,1366	0,0017	1,243	0,037	0,0660	0,0018	0,423	825	10	806	57	-2
*8.2	core	680	227	0,33	84,2	0,000033	0,06	0,1441	0,0015	1,340	0,017	0,0674	0,0004	0,857	868	9	851	13	-2
9,1	osc.-zoned outer	181	85	0,47	21,8	0,000195	0,34	0,1396	0,0017	1,275	0,028	0,0663	0,0012	0,562	842	10	814	38	-3
10,1	osc.-zoned outer	121	66	0,54	14,5	0,000162	0,28	0,1391	0,0018	1,303	0,031	0,0679	0,0013	0,555	840	10	866	41	3
11,1	core	90	45	0,50	11,0	0,000500	0,87	0,1402	0,0021	1,282	0,056	0,0663	0,0027	0,349	846	12	817	86	-3
12,1	osc.-zoned outer	175	89	0,51	21,4	0,000157	0,27	0,1414	0,0018	1,347	0,031	0,0691	0,0013	0,548	853	10	901	39	6
13,1	core	122	71	0,58	14,5	0,000390	0,68	0,1379	0,0018	1,251	0,046	0,0658	0,0023	0,353	833	10	799	72	-4
14,1	core	551	210	0,38	67,7	0,000085	0,15	0,1428	0,0016	1,302	0,018	0,0661	0,0006	0,770	861	9	810	19	-6
*15.1	osc.-zoned outer	91	46	0,51	10,5	0,000330	0,57	0,1340	0,0025	1,230	0,043	0,0666	0,0019	0,539	811	14	825	61	2
*16.1	osc.-zoned outer	167	88	0,53	19,0	0,000544	0,95	0,1310	0,0016	1,165	0,044	0,0645	0,0023	0,330	794	9	758	76	-5
*17.1	core	1060	549	0,52	132,3	0,000025	0,04	0,1452	0,0016	1,345	0,017	0,0672	0,0004	0,880	874	9	843	13	-4
18,1	osc.-zoned outer	173	75	0,43	20,7	0,000280	0,49	0,1382	0,0017	1,225	0,035	0,0643	0,0017	0,427	834	10	752	55	-10
18,2	core	910	470	0,52	109,2	0,000029	0,05	0,1396	0,0016	1,304	0,017	0,0678	0,0004	0,886	842	9	862	13	2
19,1	weakly zoned outer	113	44	0,39	14,0	0,000101	0,18	0,1442	0,0019	1,328	0,030	0,0668	0,0012	0,588	868	11	831	38	-4
20,1	osc.-zoned outer	157	65	0,42	18,9	0,000278	0,48	0,1394	0,0020	1,285	0,038	0,0669	0,0017	0,484	841	11	833	54	-1
*21.1	osc.-zoned outer	148	82	0,56	18,6	0,000078	0,13	0,1465	0,0021	1,389	0,032	0,0688	0,0012	0,621	881	12	891	37	1
22,1	osc.-zoned outer	97	51	0,53	11,4	0,000114	0,20	0,1366	0,0019	1,265	0,033	0,0672	0,0015	0,523	825	11	843	46	2
23,1	osc.-zoned outer	151	78	0,52	18,1	0,000168	0,29	0,1393	0,0019	1,266	0,030	0,0659	0,0013	0,586	841	11	803	40	-4
24,1	osc.-zoned outer	137	78	0,57	16,7	0,000104	0,18	0,1418	0,0018	1,293	0,036	0,0661	0,0016	0,474	855	10	811	51	-5

Grain. spot	Zircon type	U (ppm)	Th (ppm)	Th/U	Pb* (ppm)	$^{204}Pb/^{206}Pb$	f_{206} %	$^{206}Pb/^{238}U$	±	$^{207}Pb/^{235}U$	±	$^{207}Pb/^{206}Pb$	±	ρ	$^{206}Pb/^{238}U$	±	$^{207}Pb/^{206}Pb$	±	% Disc
MAZ-6037 (continued)																			
25,1	osc.-zoned outer	163	80	0,49	20,1	0,000083	0,14	0,1432	0,0018	1,340	0,033	0,0679	0,0014	0,503	863	10	864	44	0
26,1	osc.-zoned outer	135	79	0,58	16,7	0,000264	0,46	0,1438	0,0020	1,296	0,038	0,0654	0,0017	0,485	866	11	787	53	-9
27,1	osc.-zoned outer	325	131	0,40	38,7	0,000147	0,26	0,1383	0,0016	1,258	0,021	0,0660	0,0008	0,685	835	9	807	25	-3
	Error in FC1 reference zircon calibration was 0.40%, not included in above errors but required when comparing $^{206}Pb/^{238}U$ data from different analytical sessions.																		
ESP-7066																			
*1.1	osc.-zoned	279	18	0,07	42,3	0,000034	0,06	0,1768	0,0020	1,795	0,023	0,0736	0,0005	0,863	1049	11	1031	13	-2
*1.2	weakly zoned, late	305	129	0,42	53,3	0,000002	<0.01	0,2034	0,0022	2,255	0,027	0,0804	0,0004	0,896	1193	12	1207	10	1
2,1	weakly zoned	259	48	0,18	31,0	0,000125	0,22	0,1391	0,0015	1,269	0,021	0,0662	0,0008	0,663	840	9	812	26	-3
2,2	weakly zoned, late	111	56	0,51	13,5	0,000335	0,59	0,1421	0,0017	1,319	0,022	0,0673	0,0007	0,738	857	11	847	23	-1
3,1	weakly zoned, late	828	161	0,19	98,4	0,000014	0,02	0,1384	0,0014	1,282	0,014	0,0672	0,0003	0,918	836	8	843	9	1
*4.1	embayed overgrowth	530	8	0,01	30,5	0,000118	0,21	0,0669	0,0007	0,510	0,008	0,0553	0,0006	0,715	417	4	425	24	2
4,2	osc.-zoned	421	209	0,50	50,5	0,000070	0,12	0,1395	0,0015	1,302	0,016	0,0677	0,0004	0,880	842	9	859	12	2
5,1	zoned tip	271	139	0,51	31,8	0,000196	0,34	0,1369	0,0015	1,284	0,017	0,0680	0,0005	0,841	827	9	870	15	5
6,1	weakly zoned outer	539	192	0,36	64,1	0,000000	<0.01	0,1385	0,0015	1,285	0,015	0,0673	0,0004	0,885	836	8	846	12	1
*7.1	embayed overgrowth	525	9	0,02	30,8	0,000060	0,11	0,0683	0,0008	0,523	0,010	0,0556	0,0009	0,567	426	5	434	36	2
8,1	zoned tip	181	113	0,62	21,9	0,000048	0,08	0,1409	0,0016	1,321	0,024	0,0680	0,0009	0,649	849	9	870	28	2
*3.2	zoned core	185	90	0,49	41,5	0,000013	0,02	0,2617	0,0030	3,347	0,044	0,0927	0,0006	0,864	1499	15	1483	13	-1
*10.1	weakly zoned, late	269	75	0,28	27,8	0,000030	0,05	0,1201	0,0013	1,093	0,019	0,0660	0,0009	0,642	731	8	807	28	9
11,1	weakly zoned, late	145	36	0,25	17,1	0,000008	0,01	0,1377	0,0016	1,275	0,020	0,0671	0,0007	0,739	832	9	842	22	1
*12.1	weakly zoned, late	672	57	0,08	93,7	0,000008	0,01	0,1623	0,0017	1,614	0,018	0,0721	0,0003	0,916	970	9	988	9	2
*13.1	patchy zoning, round	587	33	0,06	87,6	0,000013	0,02	0,1737	0,0018	1,753	0,021	0,0732	0,0004	0,892	1033	10	1019	11	-1
14,1	osc.-zoned core	45	31	0,68	5,4	0,000445	0,78	0,1401	0,0022	1,279	0,034	0,0662	0,0014	0,598	845	14	813	44	-4
	Error in FC1 reference zircon calibration was 0.16%, not included in above errors but required when comparing $^{206}Pb/^{238}U$ data from different analytical sessions.																		

Notes :

1. Uncertainties given at the 1σ level.
2. f_{206} % denotes the percentage of ^{206}Pb that is common Pb.
3. Correction for common Pb made using the measured $^{204}Pb/^{206}Pb$ ratio.
4. For % Disc., 0% denotes a concordant analysis.
5. Asterisk indicates data not used in calculation Concordia age as in Ludwig (2001)